CERN - EUROPEAN ORGANIZATION FOR NUCLEAR RESEARCH

Invited Talk presented at the
Topical Conference on Baryon
Resonances, Oxford 5-9 July 1976

CERN/EP/PHYS 76-51
10 August 1976

K^-d Interactions Around 1660 MeV and an Energy Dependent $\bar{K}N \to \Sigma\pi$ Partial Wave Analysis

V. Hepp
CERN, European Organization for Nuclear Research, Geneva

O. Braun, H.J. Grimm, H. Ströbele, C. Thöl, T.J. Thouw
Institut für Hochenergiephysik, Heidelberg

D. Capps, F. Gandini, C. Kiesling, D.E. Plane and W. Wittek
Max-Planck-Institut, München

Presented by V. Hepp

ABSTRACT

Results of a K^-d bubble chamber experiment based on a statistics of 5.2 events/μb are reported. Two-and three-body K^-n and K^-p reactions were measured at incident K^- momenta between 686 and 844 MeV/c. A partial wave analysis of $\bar{K}N \to \Sigma\pi$ was performed, and an acceptable solution using only "well established" resonances was found. Some results on K^-d reactions in which both nucleons take part are presented.

1. K^-n and K^-p reactions in deuterium

Results of a K^-d experiment in the $\bar{K}N$ energy range between 1600 and 1740 MeV are presented. The 81 cm Saclay deuterium bubble chamber was exposed to a K^- beam at 4 momenta (686, 738, 788 and 844 MeV/c) at the CERN PS. About 220 000 events of all topologies were analysed, corresponding to a sample-size of 5 200 events/mb. The aim of the experiment was to clarify the confused resonance structure in the Σ(1660) region by measuring the I = 1 $\bar{K}N$ amplitudes with good precision.

The following reactions were studied:

i) $K^-d \to \Lambda\pi^-p$, $\Sigma^0\pi^0p$, $\Lambda\pi^-\pi^0p$, $\Sigma\pi\pi p$, $N\bar{K}\pi^-p$

ii) $K^- d \to \Sigma^{\pm}\pi^{\mp} n$, $\Lambda\pi^+\pi^- n$, $p\bar{K}^0\pi^- n$

iii) $K^- d \to \Sigma^- p$, $\Sigma^{-*}(1385)p$, $\Lambda^*(1405)n$

Reactions i) are $K^- n$ interactions, ii) are $K^- p$ reactions and iii) are processes in which both nucleons take part in the interaction. The reactions $K^- d \to K^- d$, $K^- pn$ are under study.

$K^- n$ and $K^- p$ cross sections were extracted by treating the nucleons in the deuteron in the usual Hulthén approximation. A cut in the spectator momentum at 300 MeV/c was imposed.

For all two body $Y\pi$ final states differential cross sections were measured. The polarizations in $K^- n \to \Lambda\pi^-$ and $K^- n \to \Sigma^0\pi^-$ were also determined. The corresponding A_i and B_i coefficients were calculated by the method of moments.

In various checks of the data internal consistency and agreement with other experiments was found. In particular, the cross sections and angular distributions for the $K^- p$ reactions ii), as measured in deuterium, were found to be consistent with the corresponding hydrogen data. Only the cross section for $K^- d \to \Sigma^+\pi^- n$ appeared to be low by $\lesssim 15\%$ compared to $K^- p \to \Sigma^+\pi^-$ [1], [2] which we attribute to YN final state interactions in deuterium. The reaction $K^- n \to \Lambda\pi^-$ was compared to $K^- p \to \Lambda\pi^0$ [1], [2], being related by isospin invariance. Good agreement in cross sections, angular distributions and polarizations was obtained.

In figs 1a) and 1d) the two-body cross sections: $\sigma(K^- n \to \Sigma^-\pi^0)$, $\sigma(K^- n \to \Sigma^0\pi^-)$, $\sigma(K^- n \to \Lambda\pi^-)$ and $\sigma(K^- n \to \Sigma^-\pi^0 + \Sigma^0\pi^-)$ are shown. Also indicated in fig. 1c) is $2 * \sigma(K^- p \to \Lambda\pi^0)$ (open circles). Of the three-body cross sections we show for example $\sigma(K^- n \to \Sigma\pi\pi)$ and $\sigma(K^- n \to \Lambda\pi\pi)$ in fig. 2. The formation of $\Sigma(1660)$ is clearly seen in fig. 1d), 2a) and 2c).

In fig. 3 a comparison of our measurements for $K^- p \to \Lambda\pi^+\pi^-$ and $p\bar{K}^0\pi^-$ with hydrogen data (open circles) is made. The cross section $\sigma(\bar{K}N \to \Lambda\pi\pi, I = 0)$ can be calculated from $\sigma(K^- p \to \Lambda\pi^+\pi^-)$ and $\sigma(K^- n \to \Lambda\pi^-\pi^0)$ and is shown in fig. 4. A structure at $E^* \sim 1675$ MeV indicates $\Lambda(1670)$ and/or $\Lambda(1690)$ formation in the three-body final state.

2. Partial Wave Analysis of $\bar{K}N \to \Sigma\pi$

The data from the reactions $K^- n \to \Sigma^{\circ}\pi^{\circ}$ were averaged (same I = 1 amplitude) and were used for an energy dependent partial wave analysis in the somewhat enlarged energy range: $1522 \leq E^* \leq 1747$ MeV. In addition to our data, measurements on $K^- p \to \Sigma^{\pm}\pi^{\mp}$, $K^- p \to \Sigma^{\circ}\pi^{\circ}$ and $\bar{K}^{\circ} p \to \Sigma^{\circ}\pi^{+}$ were used (in total 875 data points) [1,2,5,9 and 10].

The amplitudes were parametrized as follows:

$$T = T_{RES} + T_{BG}$$

$$T_{RES} = \frac{t}{\epsilon - i} e^{i\phi}, \quad \epsilon = \frac{2}{\Gamma(E)} (E_{RES} - E)$$

$$T_{BG} = A*P_o(E') + B*P_1(E') + C*P_2(E')$$

P_o, P_1, P_2 are Legendre Polynomials and the argument E' was chosen as:

$$E' = (2E - E_{max} - E_{min})/(E_{max} - E_{min}), \quad \begin{matrix} E_{min} = 1522 \text{ MeV} \\ E_{max} = 1747 \text{ MeV} \end{matrix}$$

For the resonant amplitude t the sign convention of [11] was adopted.

In the search for acceptable solutions we tried to keep the number of resonances as small as possible. The resonance parameters of $\Lambda(1520, 3/2^-)$, $\Sigma(1765, 5/2^-)$, $\Lambda(1815, 5/2^+)$ and $\Lambda(1830, 5/2^-)$ at the edges of the chosen energy interval were kept fixed.

We found that only the three well established resonances $\Lambda(1670, 1/2^-)$, $\Sigma(1660, 3/2^-)$ and $\Lambda(1690, 3/2^-)$ were necessary and sufficient for an acceptable fit of the data. In these partial waves a background of up to 1st order Legendre Polynomials was allowed. The remaining waves: S11, P01, P11, P03, P13 were parametrised in terms of 2nd order Legendre Polynomials.

Our best solution is characterised by a χ^2 of 1199 for 821 degrees of freedom, corresponding to a χ^2 per data point of 1.46. Table 1 gives the fitted values for the resonance parameters and background coefficients. Parameters in brackets were kept fixed. The errors on the resonance

parameters indicate the spread of values obtained in our different fits. We note that various searches with additional resonances in the S and P waves did not improve substantially the fit.

It is pointed out that our $K^- n \to (\Sigma\pi)^-$, I = 1 cross sections are considerably smaller than $\sigma(\bar{K}^o p \to \Sigma^o \pi^+)$ from $K_L p$ experiments [6,7,8 and 9]. Fig. 5 is a compilation of measured [3,4,6,7,8 and 9] and predicted I = 1 $(\Sigma\pi)^\pm$ cross sections [1,2,5 and 10].

The discrepancy between $K^- n \to (\Sigma\pi)^-$ and $\bar{K}^o p \to \Sigma^o \pi^+$ can only partly be explained by final state interactions in deuterium (ΣN scattering). If we scale our cross sections by 1.15, i.e. by taking the suppression of the $K^- d \to \Sigma^+ \pi^- n$ cross section, mentioned above, as an upper limit for final state interactions in the $(\Sigma\pi)^-$ channels, our solution remains the same within the quoted errors.

Fig. 6 shows part of our input data, namely the cross sections for $K^- p \to \Sigma^\pm \pi^\mp$, $K^- p \to \Sigma^o \pi^o$, $K^- n \to (\Sigma\pi)^-$ and the data point for $\bar{K}^o p \to \Sigma^o \pi^+$ of ref. [9] (triangle in fig. 6b) used in our fit. Fig. 7 displays the shape coefficients A_i/A_o and B_i/A_o for the $(\Sigma\pi)^\pm$ final state. The solid curves in figs 6 and 7 represent our solution, the dashed curves are the solution of the RL-IC fit [12] which was also presented at this conference. A major discrepancy is seen for $A_o(\Sigma\pi)^\pm$ and $A_o(\Sigma^o\pi^o)$ which results from the different choice of input data in the two analyses. The RL-IC group used $K_L p \to \Sigma^o \pi^+$ data from ref. [6] for the I = 1 $(\Sigma\pi)$ final state and omitted the cross section data on $K^- p \to \Sigma^o \pi^o$ [1,2 and 5].

Fig. 8 shows the Argand diagrams of the two analysis. The solid curves correspond to our solution, the dashed curve to RL-IC. As expected, the amplitudes for the I = 0 partial waves are lower in the RL-IC fit than in our solution. The reverse is true for the I = 1 amplitudes. Note that the S11, P01 and P11 waves had been parametrized as resonances in the RL-IC analysis.

It is likely that at the present stage the inconsistencies in the data are more important than refinements in the adopted models. We therefore consider a χ^2 of 1.46 per data point as adequate.

3. $\bar{K}d$ interactions

In a study of $\bar{K}d$ interactions in which both nucleons take part, we obtained the following results, using all 4 incident momenta:

- From a sample of 260 events of $\bar{K}d \to \Sigma^- p$ a cross section of $\sigma_{\Sigma^- p} = (69 \pm 4)\mu b$ is obtained.
- In the reaction $\bar{K}d \to \Lambda\pi^- p$ the "formation" of $\Sigma(1385)$ is observed (fig. 9). From 441 events in the resonance we find for the cross section $\sigma(\bar{K}d \to \Sigma(1385)^- p)$: $\sigma_{\Sigma^* p} = (160 \pm 15)\ \mu b$
- We observe "formation" of $\Lambda(1520)$ and $\Lambda(1405)$ in $\bar{K}d \to \Sigma^-\pi^+ n$ (fig. 10). We estimate for the cross section $\sigma(\bar{K}d \to \Lambda(1405)n)$:

$$\sigma_{\Lambda^* n} = (250 \pm 50)\ \mu b.$$

- A narrow enhancement [13] in the effective (1p) mass occurs in the reaction $\bar{K}d \to \Lambda\pi^- p$ at low ($K\pi$) momentum transfers (fig. 11). A fit to an S-wave Breit-Wigner mass dependence yields:

$$M = 2129.0 \pm 0.5\ \text{MeV}$$
$$\Gamma = 5.4 \pm 1.7\ \text{MeV}$$

The enhancement is very close to $\Sigma^+ n$ threshold.

4. Summary

a) In a high statistics deuterium experiment $\bar{K}p$ and $\bar{K}n$ reactions were measured simultaneously at CMS energies between 1.60 and 1.74 GeV. Systematic errors due to final state interactions are estimated to be $\lesssim 15\%$. The cross sections for the I = 1 reactions $\bar{K}n \to (\Sigma\pi)^-$ are found to be much smaller than the corresponding $\bar{K}^0 p \to \Sigma^0\pi^+$ cross sections, obtained in $K_L p$ experiments. The same discrepancy occurs for the ratio:

$\bar{K}n \to \Sigma^-\pi^+\pi^-/\bar{K}n \to \Sigma^+\pi^-\pi^-$ compared to: $K_L p \to \Sigma^+\pi^-\pi^+/K_L p \to \Sigma^-\pi^+\pi^+$.

b) The three-body decay modes [$\Sigma\pi\pi$, $\Lambda\pi\pi$] of $\Sigma(1660)$ were found to be small. The $\Sigma(1660)$ resonance as seen in formation experiments might be identified with the $\Sigma(1660)$ resonance of production experiments produced at large momentum transfers.

c) A partial wave analysis of $\bar{K}N \to \Sigma\pi$ gave an acceptable fit, using "well established" resonances only.

d) "Formation" of $\Sigma^-(1197)$, $\Sigma^{-*}(1385)$ and $\Lambda^*(1405)$ below $\bar{K}N$ threshold is observed and cross sections are given. The existence of a very narrow Λp enhancement near $\Sigma^+ n$ threshold is demonstrated.

References

[1] R. Armenteros et al., Nucl. Phys. B8 (1968) 233.

[2] R. Armenteros et al., Nucl. Phys. B21 (1970) 15.

[3] R. Armenteros et al., Nucl. Phys. B10 (1969) 459.

[4] R. Armenteros et al., Nucl. Phys. (1970) 425.

[5] R.D. Tripp, private communication (1976).

[6] L. Bertanza et al., (BEGPR-College) Rutherford Laboratory, prep. RL-76-016 (1976).

[7] E. Burkhardt et al., Nucl. Phys. B99 (1975) 365.

[8] R.J. Yarmartino et al., Phys. Review D10 (1974) 9.

[9] Y. Cho et al., Phys. Letters 60B (1976) 293.

[10] M. Jones et al., Nucl. Phys. B90 (1975) 345.

[11] R.D. Tripp et al., Phys. Review Letters 21 (1968) 172.

[12] G.P. Gopal et al., Rutherford Laboratory prep. RL-75-182 (1975).

[13] For further reference see: D. Eastwood et al., Phys. Review D3 (1971) 2603.

CERN/EP/PHYS 76-51

TABLE I

FITTED VALUES FOR THE RESONANCE PARAMETERS AND BACKGROUND COEFFICIENTS. THE PARAMETERS WITHIN SQUARE BRACKETS WERE KEPT FIXED

RESONANCES					Characteristics of the fit
Partial wave	Mass [MeV]	Width [MeV]	Resonant Amplitude	phase [rad]	
S01	1676 ± 2	43 ± 5	-0.29 ± 0.03	-0.06	No. of data points 875
D03	[1519]	[16]	[0.46]	[0.]	
D03	1688 ± 3	76 ± 8	-0.30 ± 0.03	0.08	No. of parameters 54
D13	1669 ± 6	53 ± 3	0.20 ± 0.01	0.30	No. of degrees of freedom 821
D05	[1825]	[94]	[-0.15]	[0.]	
D15	[1764]	[123]	[0.10]	[0.]	χ^2 1199
F05	[1820]	[83]	[-0.27]	[0.]	χ^2/ND 1.46

BACKGROUND						
Partial wave	Re(A)	Im(A)	Re(B)	Im(B)	Re(C)	Im(C)
S01	-0.266	0.136	0.100	-0.111	-	-
S11	0.058	0.253	-0.035	-0.114	0.043	-0.011
P01	0.070	-0.225	0.153	-0.049	-0.045	0.091
P11	0.003	-0.099	0.043	-0.069	-0.014	0.008
P03	0.104	0.079	0.050	0.019	0.015	-0.053
D13	0.081	0.007	-0.002	-0.005	0.024	-0.000
D03	-0.016	-0.032	0.025	0.013	-	-
D13	-0.024	-0.014	-0.000	-0.033	-	-

Figure Captions

Fig. 1 Cross sections for 2 body reactions. In fig. 1c) $\sigma(K^-n \to \Lambda\pi^-)$ is compared with $2\sigma(K^-p \to \Lambda\pi^o)$ indicated by open circles [1,2].

Fig. 2 Cross sections for $K^-n \to \Sigma\pi\pi$ and $\Lambda\pi\pi$.

Fig. 3 Cross sections for $K^-p \to \Lambda\pi^+\pi^-$ and $p\bar{K}^o\pi^-$. Full circles denote our measurements in deuterium, open circles are hydrogen results ([1,2]).

Fig. 4 I = 0 cross section for $\bar{K}N \to \Lambda\pi\pi$ derived from $K^-p \to \Lambda\pi^+\pi^-$ and $K^-n \to \Lambda\pi^-\pi^o$, as measured in this experiment.

Fig. 5 Compilation of I = 1 $(\Sigma\pi)$ - cross sections divided by $4\pi\lambda\!\!\!^{-2}$. The data were taken from: CHM: this experiment; CS: [3,4]; CHS: [1,2]; LBL: [5]; BEGPR: [6]; HD-TA: [7]; SLAC: [8]; ACM: [9].

Fig. 6 Cross sections divided by $4\pi\lambda\!\!\!^{-2}$ as function of $\bar{K}N$ energy for the reactions:
a) $\bar{K}^-p \to \Sigma^+\pi^-$ [1,2,5 and 10]; b) $K^-n \to (\Sigma\pi)^-$, this experiment, and $\bar{K}^op \to \Sigma^o\pi^+$ [9]; c) $K^-p \to \Sigma^o\pi^o$ [1,2 and 5] d) $K^-p \to \Sigma^-\pi^+$ [1,2,5 and 10].

Fig. 7 Coefficients A_i/A_o and B_i/A_o (i = 1,2,3 and 4) for $\bar{K}N \to (\Sigma\pi)^\pm$ as function of $\bar{K}N$ energy
solid curve: our solution
dashed curve: RL-IC solution [12].

Fig. 8 Argand diagrams for $\bar{K}N \to \Sigma\pi$ partial wave amplitudes.
Solid curves: our solution
dashed curves: RL-IC solution [12].

Fig. 9 Effective $(\Lambda\pi^-)$ - mass distribution in $K^-d \to \Lambda\pi^-p$. The curves show the fit for $\Sigma(1385)^-$ and background.

Figure Captions (Cont'd)

Fig. 10 Distribution of squared $(\Sigma^-\pi^+)$ effective mass in $K^-d \to \Sigma^-\pi^+n$. Formation of $\Lambda(1520)$ and $\Lambda(1405)$ can be seen.

Fig. 11 Eff. Λp-mass in $K^-d \to \Lambda\pi^-p$. Only events with small $(K^-\pi^-)$ momentum transfer were selected. The curves show the fit to a S-wave Breit-Wigner enhancement and a polynomial background.

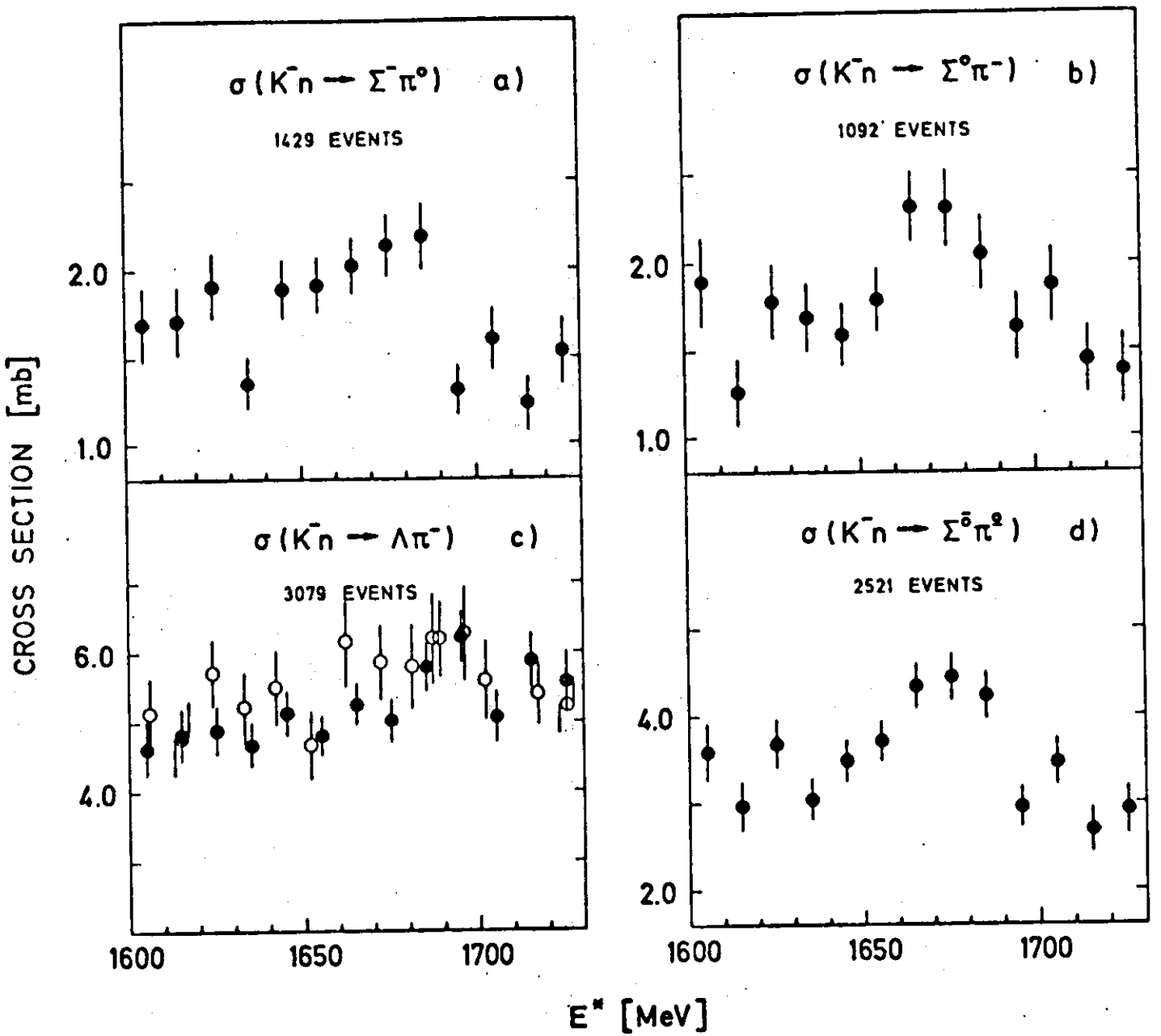
σ(K⁻n → Σ⁻π⁰) a)
1429 EVENTS
σ(K⁻n → Σ°π⁻) b)
1092 EVENTS
σ(K⁻n → Λπ⁻) c)
3079 EVENTS
σ(K⁻n → Σ⁰π⁰) d)
2521 EVENTS
CROSS SECTION [mb]
E* [MeV]
2.0
1.0
6.0
4.0
1600
1650
1700

FIG. 1

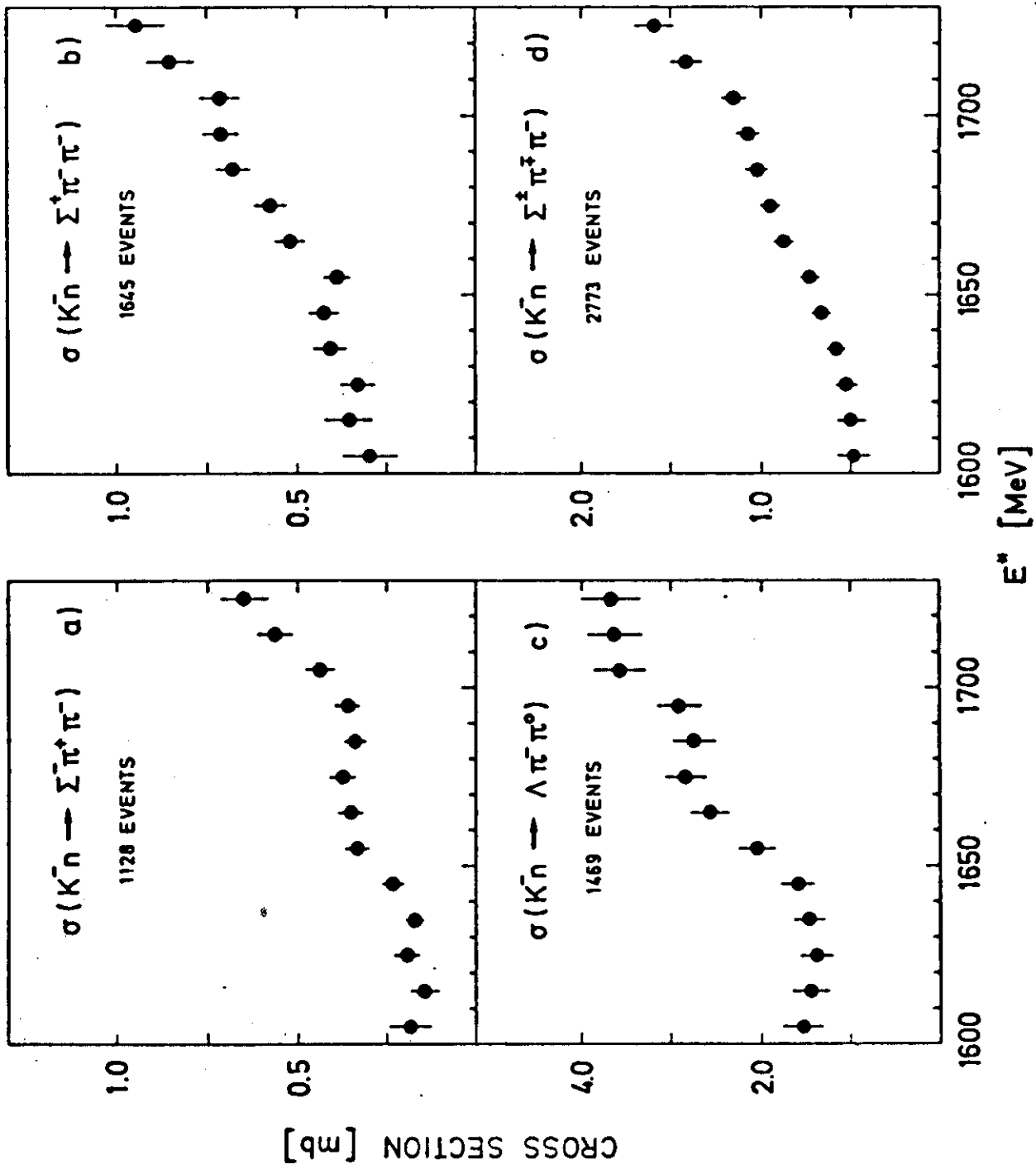
a)
σ (K⁻n → Σ⁻π⁺π⁻)
1128 EVENTS
b)
σ (K⁻n → Σ⁺π⁻π⁻)
1645 EVENTS
c)
σ (K⁻n → Λπ⁻π⁰)
1469 EVENTS
d)
σ (K⁻n → Σ±π∓π⁻)
2773 EVENTS
CROSS SECTION [mb]
E* [MeV]
1600
1650
1700
0.5
1.0
2.0
4.0

FIG.2

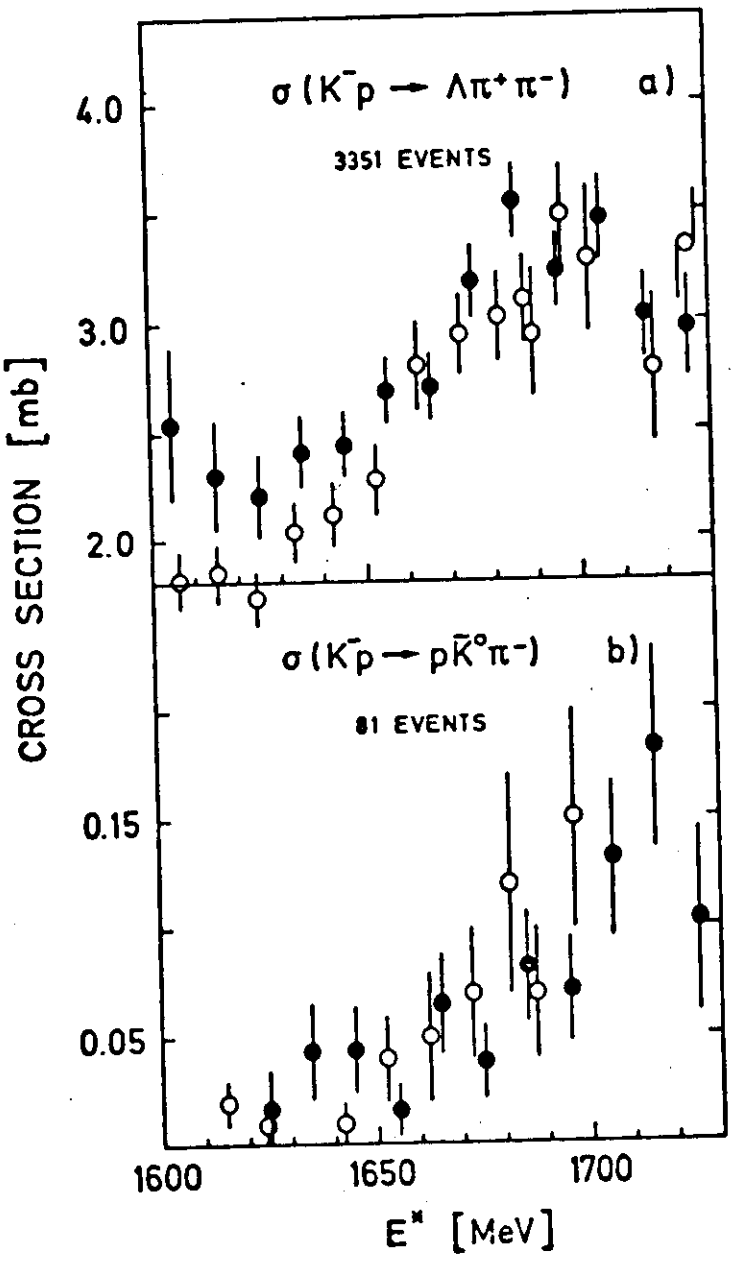
σ (K⁻p → Λπ⁺π⁻) a)
3351 EVENTS
σ (K⁻p → pK̄°π⁻) b)
81 EVENTS
CROSS SECTION [mb]
4.0
3.0
2.0
0.15
0.05
1600
1650
1700
E* [MeV]

FIG. 3

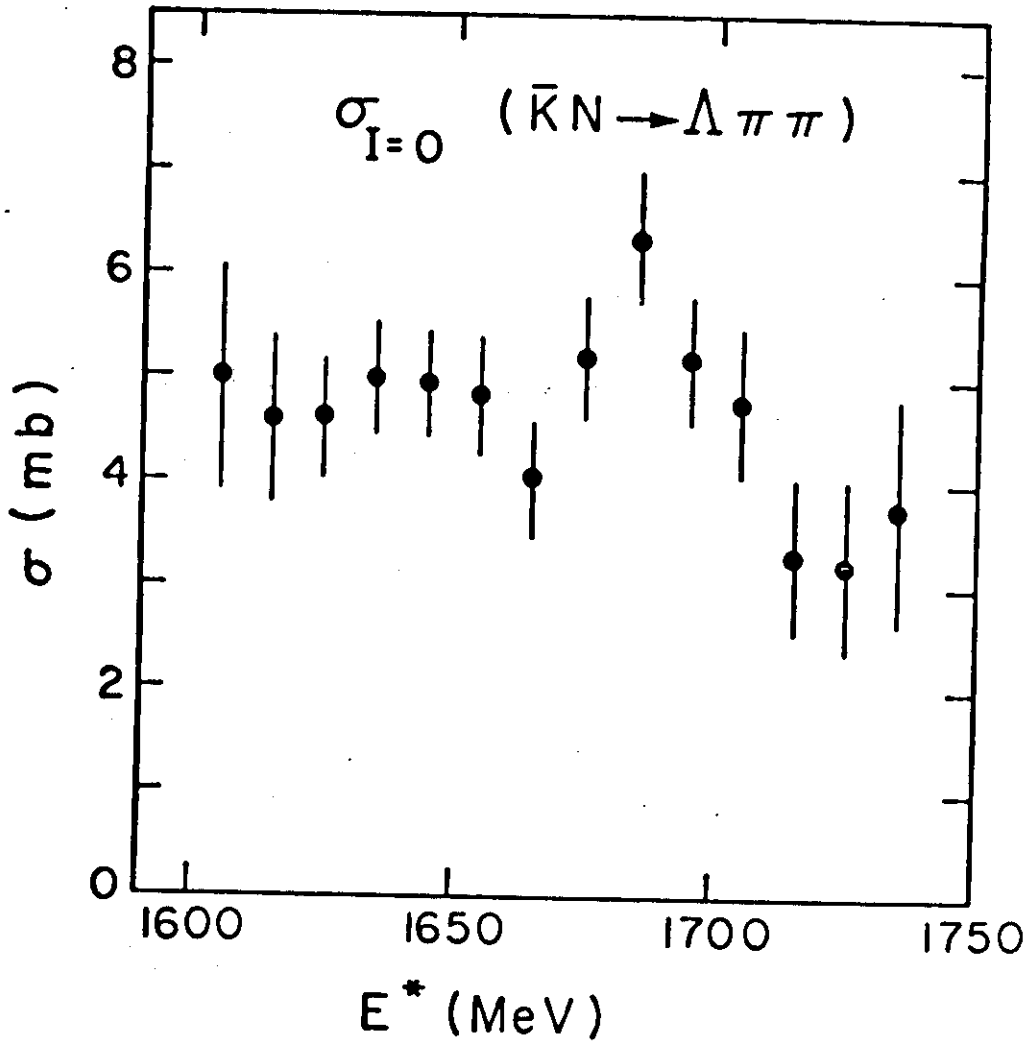
$\sigma_{I=0}$ $(\bar{K}N \rightarrow \Lambda\pi\pi)$
8
6
4
2
0
σ (mb)
1600
1650
1700
1750
E* (MeV)

FIG. 4

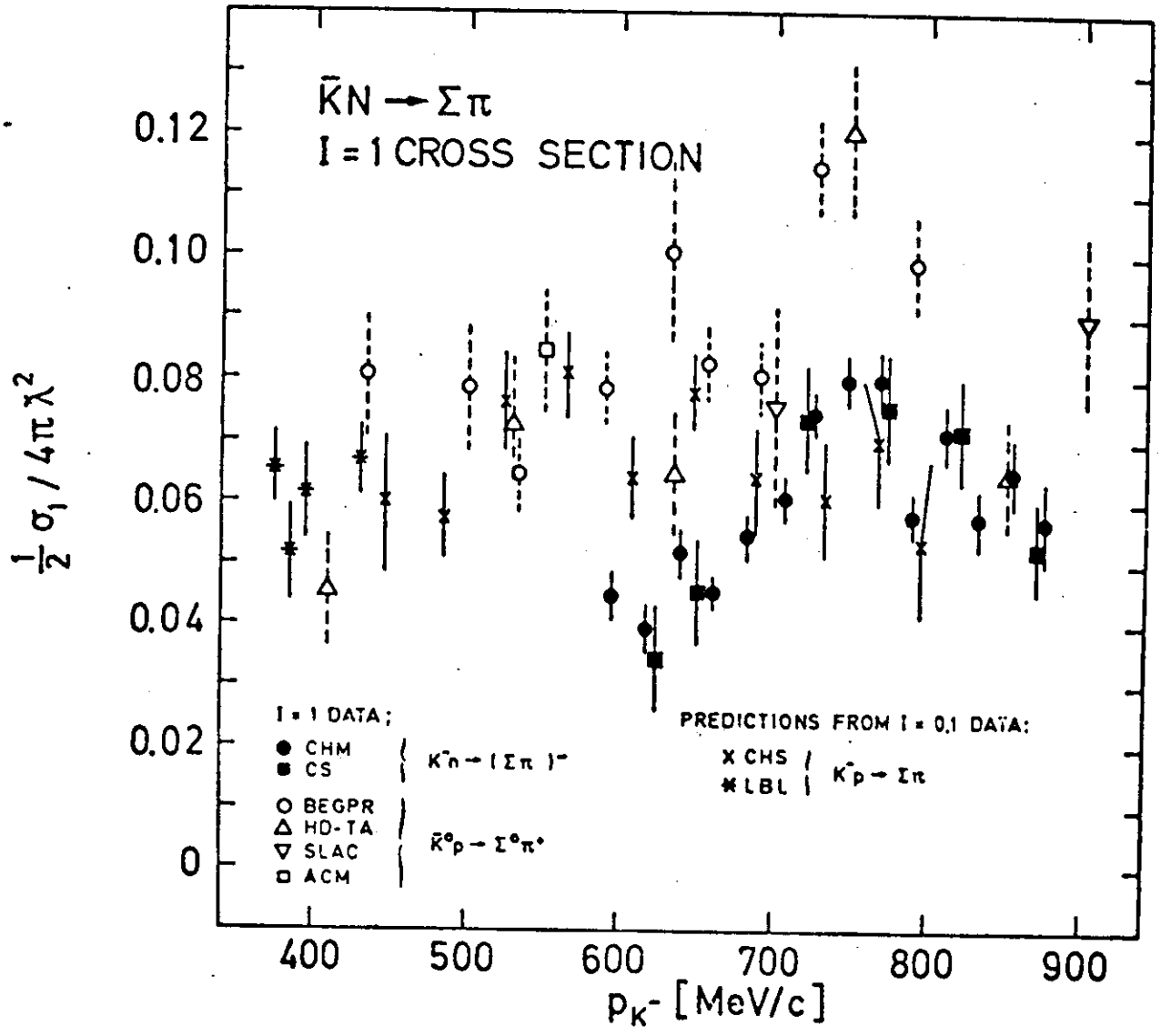
$\bar{K}N \rightarrow \Sigma\pi$
I = 1 CROSS SECTION
$\frac{1}{2}\sigma_1 / 4\pi\lambda^2$
0.12
0.10
0.08
0.06
0.04
0.02
0
400
500
600
700
800
900
p_{K^-} [MeV/c]
I = 1 DATA:
CHM
CS
$K^-n \rightarrow (\Sigma\pi)^-$
BEGPR
HD-TA
SLAC
ACM
$\bar{K}^0p \rightarrow \Sigma^0\pi^+$
PREDICTIONS FROM I = 0,1 DATA:
X CHS
* LBL
$K^-p \rightarrow \Sigma\pi$

FIG. 5

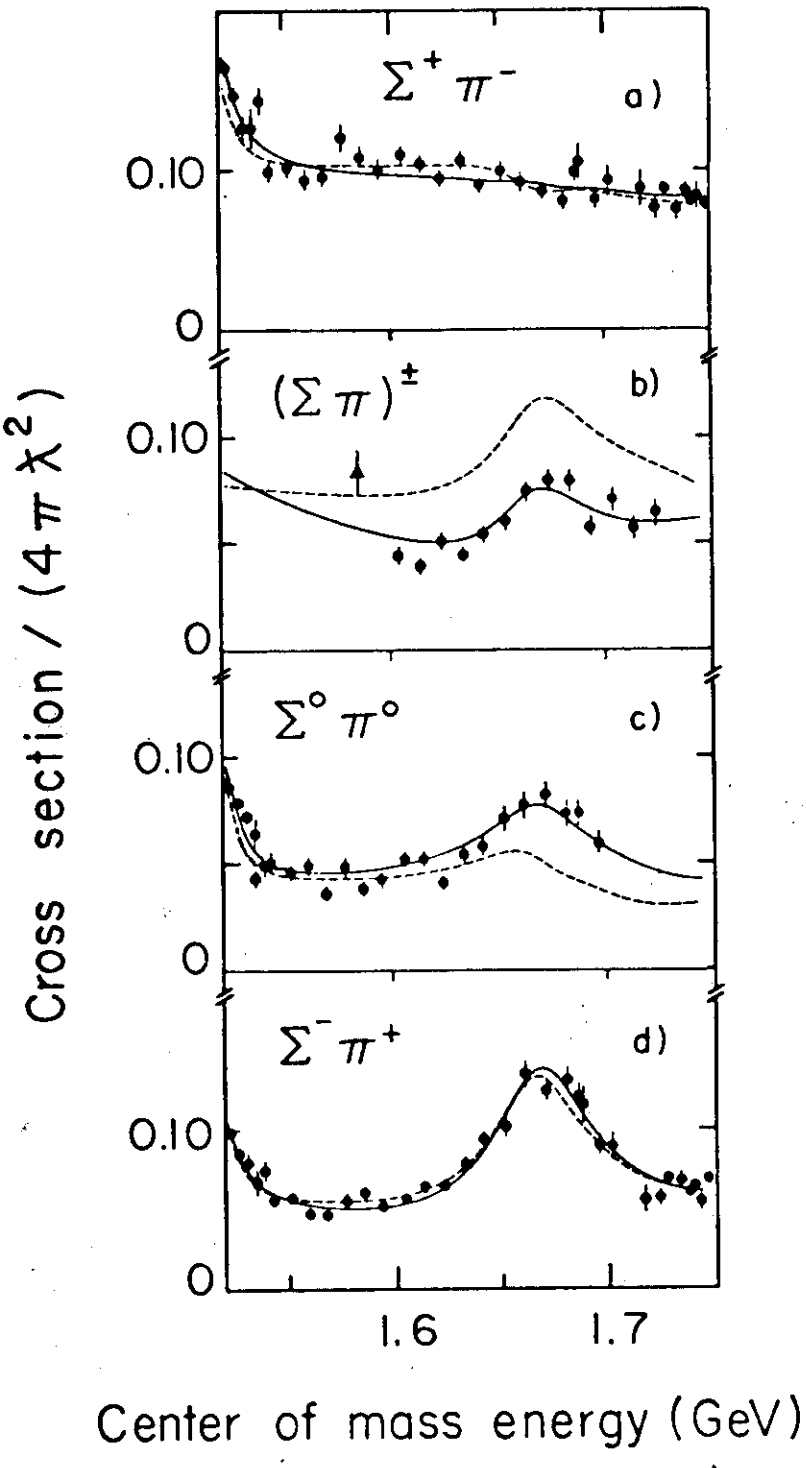
$\Sigma^+\pi^-$
a)
0.10
0
$(\Sigma\pi)^\pm$
b)
0.10
0
$\Sigma^\circ\pi^\circ$
c)
0.10
0
$\Sigma^-\pi^+$
d)
0.10
0
1.6
1.7
Cross section / $(4\pi\lambda^2)$
Center of mass energy (GeV)

FIG. 6

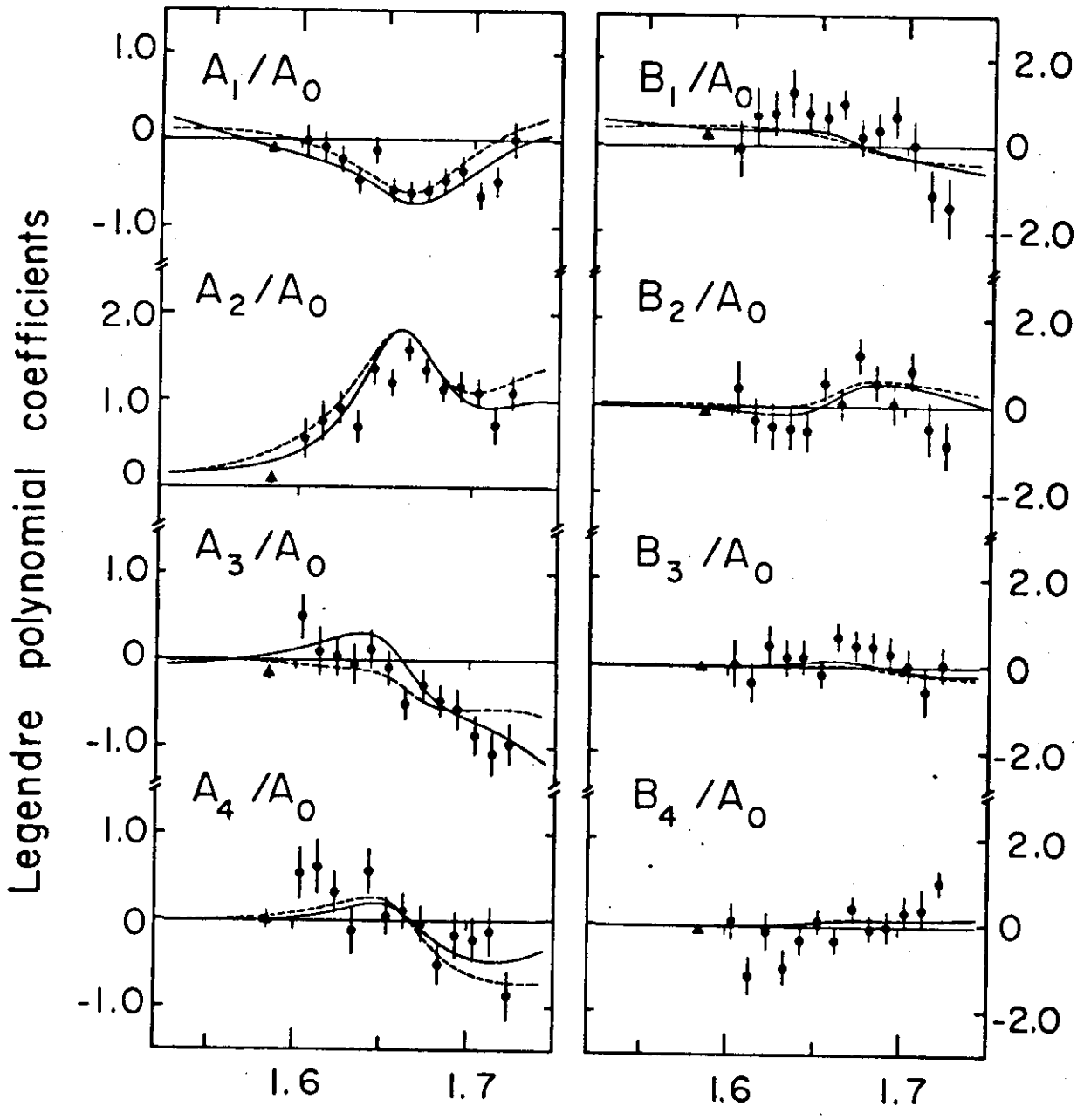
Legendre polynomial coefficients
A1/A0
A2/A0
A3/A0
A4/A0
B1/A0
B2/A0
B3/A0
B4/A0
1.0
0
-1.0
2.0
1.6
1.7
Center of mass energy (GeV)

FIG. 7

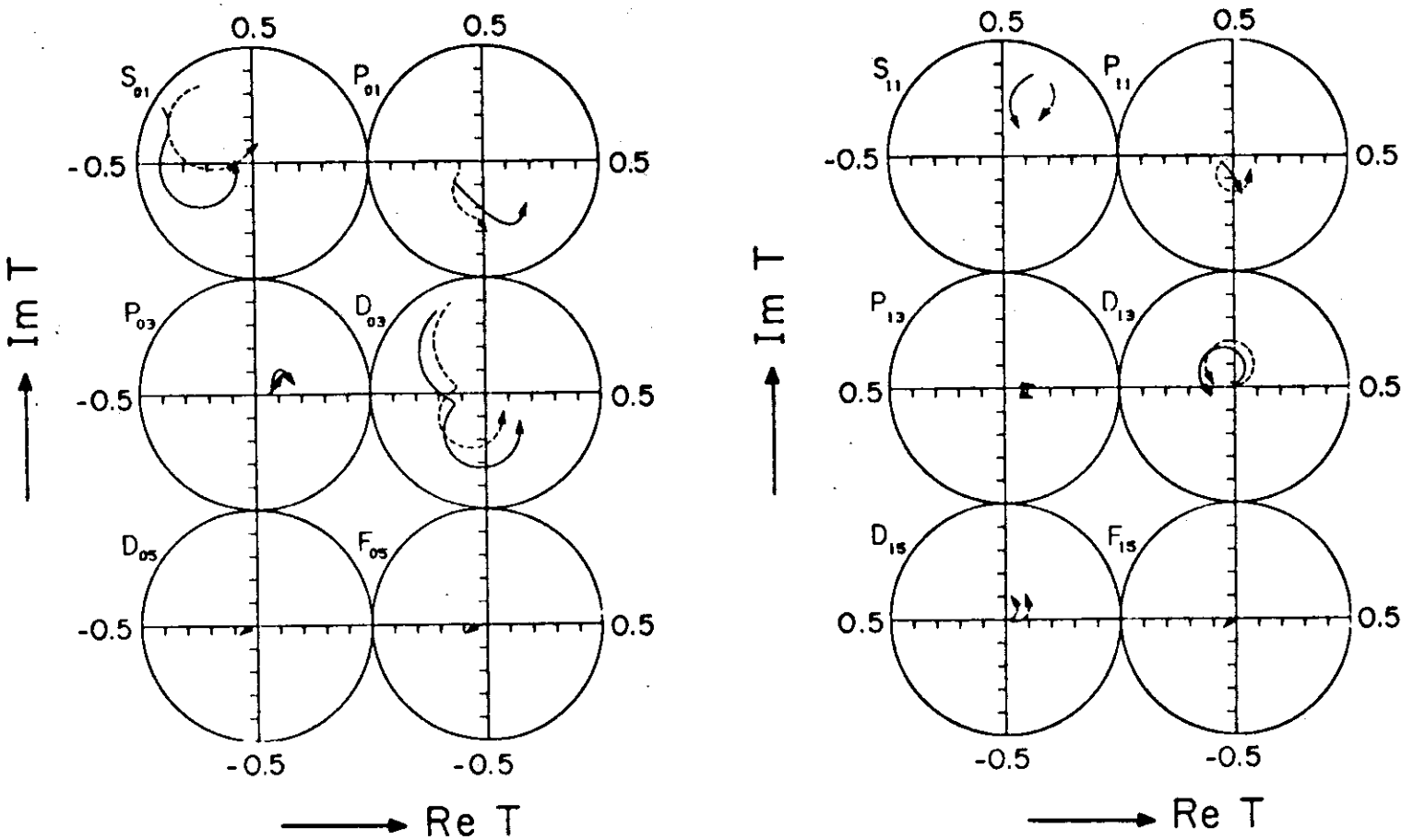
$\bar{K}N \longrightarrow \Sigma\pi$
0.5
-0.5
S_{01}
P_{01}
P_{03}
D_{03}
D_{05}
F_{05}
P_{11}
S_{11}
P_{13}
D_{13}
D_{15}
F_{15}
Im T
Re T

FIG. 8

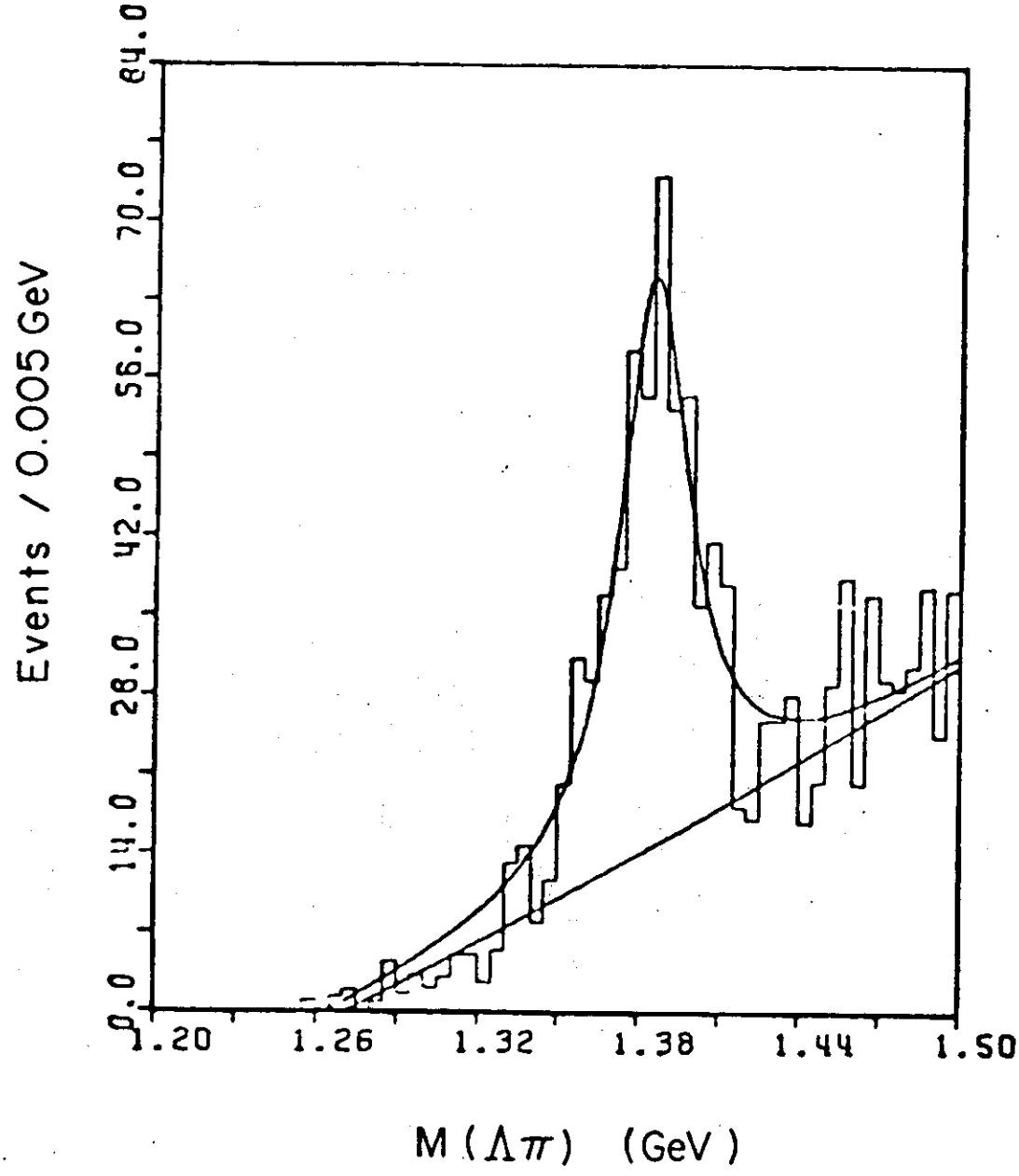
Events / 0.005 GeV
0.0
14.0
28.0
42.0
56.0
70.0
84.0
1.20
1.26
1.32
1.38
1.44
1.50
M(Λπ) (GeV)

FIG. 9

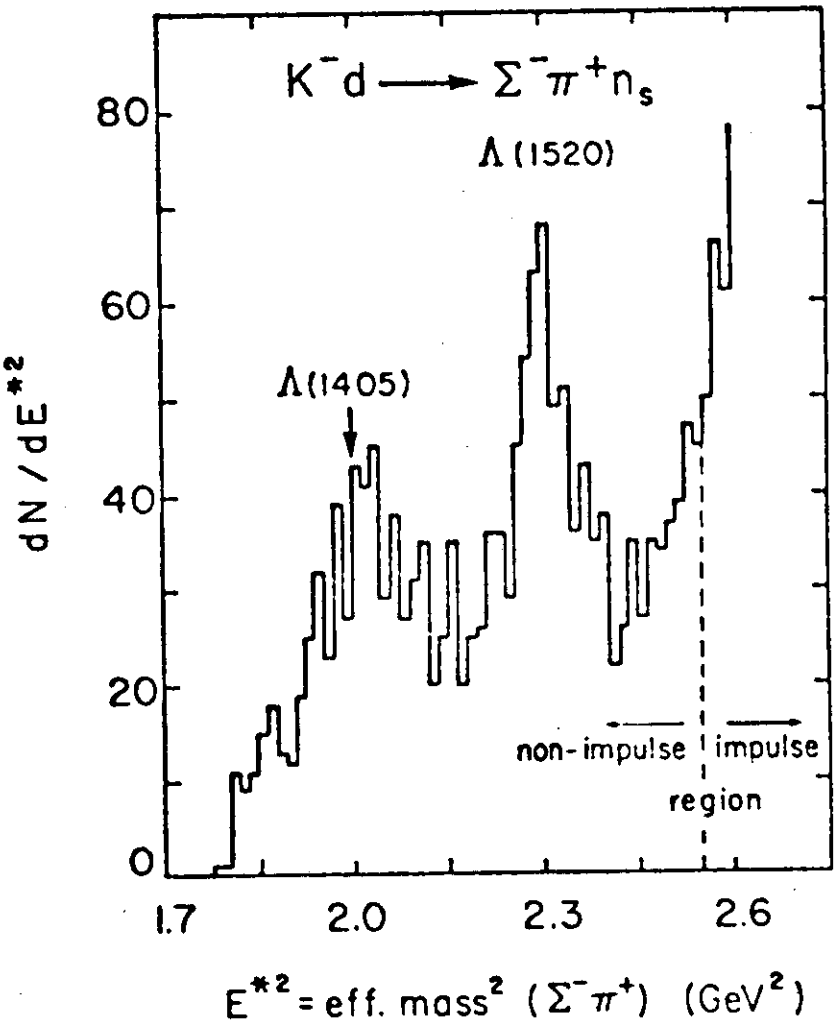
$K^- d \longrightarrow \Sigma^- \pi^+ n_s$
Λ(1520)
Λ(1405)
non-impulse
impulse
region
80
60
40
20
0
1.7
2.0
2.3
2.6
dN / dE*²
E*² = eff. mass² (Σ⁻π⁺) (GeV²)

FIG. 10

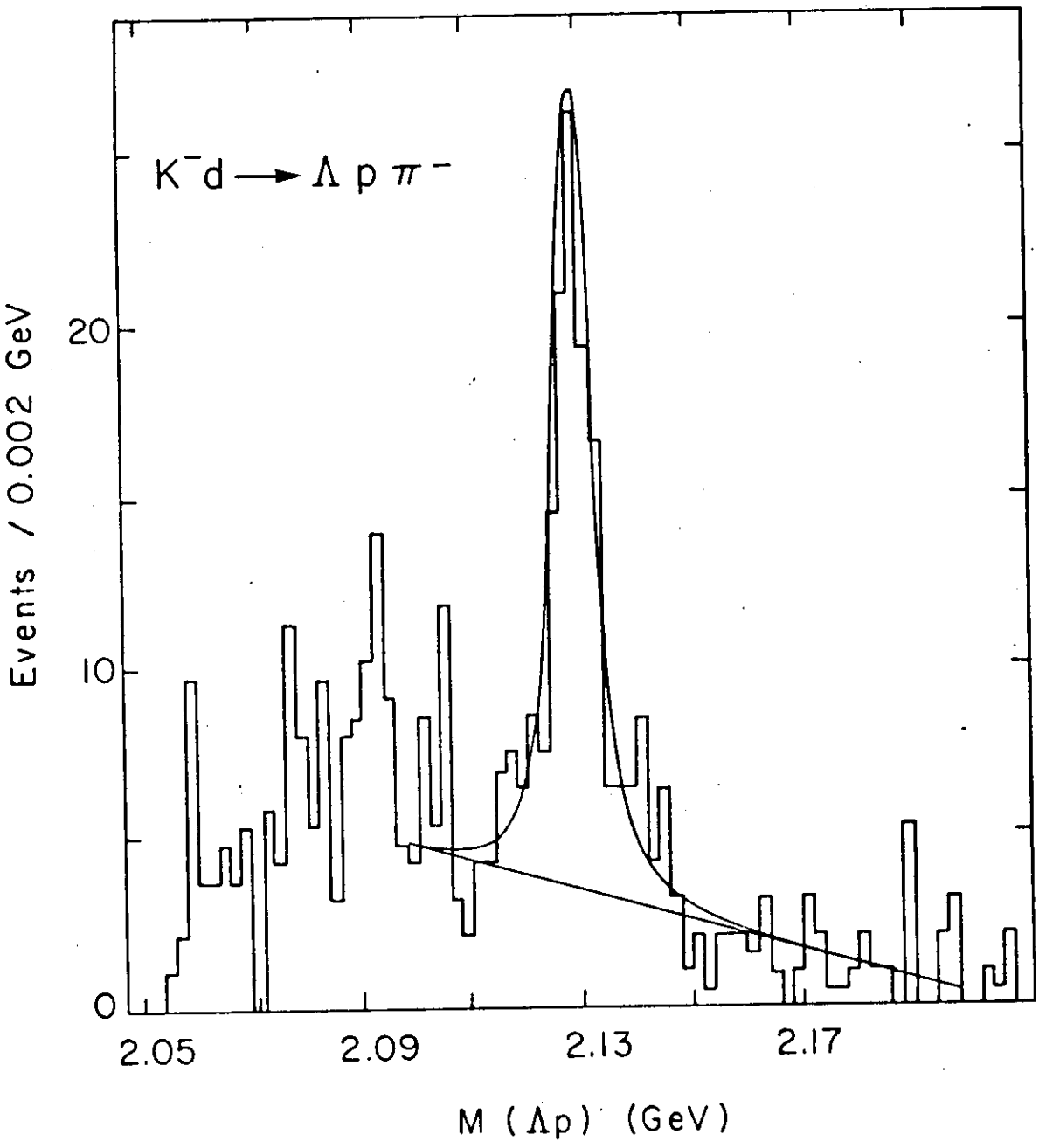
$K^- d \longrightarrow \Lambda p \pi^-$
Events / 0.002 GeV
0
10
20
2.05
2.09
2.13
2.17
M (Λp) (GeV)

FIG. 11